

# Rational Design of Hit Compounds Targeting *Staphylococcus aureus* Threonyl-tRNA Synthetase

Mariia Yu. Rybak, Olga I. Gudzera, Oksana B. Gorbatiuk, Mariia O. Usenko, Sergiy M. Yarmoluk, Michael A. Tukalo, and Galyna P. Volynets\*



Cite This: *ACS Omega* 2021, 6, 24910–24918



Read Online

ACCESS |



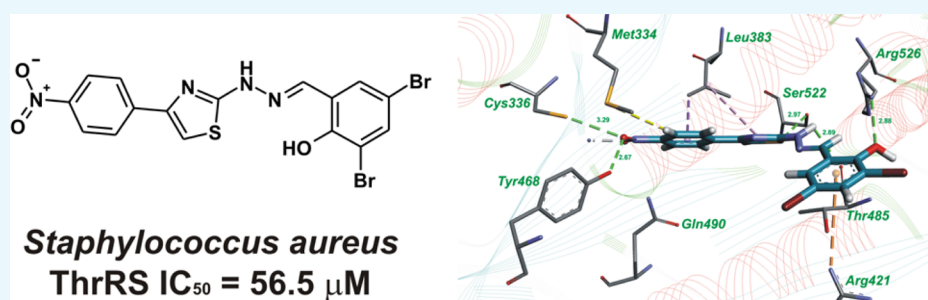
Metrics & More



Article Recommendations



Supporting Information



**ABSTRACT:** *Staphylococcus aureus* is one of the most dangerous nosocomial pathogens which cause a wide variety of hospital-acquired infectious diseases. *S. aureus* is considered as a superbug due to the development of multidrug resistance to all current therapeutic regimens. Therefore, the discovery of antibiotics with novel mechanisms of action to combat staphylococcal infections is of high priority for modern medicinal chemistry. Nowadays, aminoacyl-tRNA synthetases are considered as promising molecular targets for antibiotic development. In the present study, we used for the first time *S. aureus* threonyl-tRNA synthetase (ThrRS) as a molecular target. Recombinant *S. aureus* ThrRS was obtained in the soluble form in a sufficient amount for inhibitor screening assay. Using the molecular docking approach, we selected 180 compounds for investigation of inhibitory activity toward ThrRS. Among the tested compounds, we identified five inhibitors from different chemical classes decreasing the activity of ThrRS by more than 70% at a concentration of 100 μM. The most active compound 2,4-dibromo-6-[[4-(4-nitro-phenyl)-thiazol-2-yl]-hydrazonomethyl]-phenol has an IC<sub>50</sub> value of 56.5 ± 3.5 μM. These compounds are not cytotoxic toward eukaryotic cells HEK293 (EC<sub>50</sub> > 100 μM) and can be useful for further optimization and biological research.

## INTRODUCTION

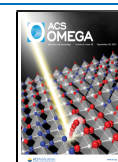
*Staphylococcus aureus* is an opportunistic Gram-positive pathogen that causes a wide range of hospital-acquired human diseases ranging from skin infections and abscesses to much more severe endocarditis, osteomyelitis, pneumonia, meningitis, sepsis, and so forth.<sup>1–8</sup> The major problem of staphylococcal infection treatment is the multidrug resistance to all antibiotics currently used in clinic, including methicillin, vancomycin, daptomycin, and linezolid.<sup>9–15</sup> Therefore, the development of antistaphylococcal agents with novel mechanisms of action is of urgent need.

Nowadays, aminoacyl-tRNA synthetases are recognized as promising molecular targets for antibiotic development.<sup>16–18</sup> Aminoacyl-tRNA synthetases are key enzymes in protein synthesis which ligate amino acids to cognate transfer RNAs being involved in the early stages of translation of the genetic code. Most living cells possess 20 aminoacyl-tRNA synthetases for each of the standard amino acids. These enzymes are divided into two classes, class I and class II, which have different folds of catalytic domain and different preferences for the hydroxyl group of the tRNA.<sup>19,20</sup> Aminoacyl-tRNA

synthetases possess some structural divergence in prokaryotic and eukaryotic organisms which increases the possibility for development of selective inhibitors toward enzymes from pathogenic microorganisms in comparison with human homologues. Aminoacyl-tRNA synthetases are conservative among bacteria, suggesting that compounds targeting these enzymes may demonstrate a wide range of antibacterial activity. A number of available crystal structures of aminoacyl-tRNA synthetases provide a basis for receptor-based drug design and virtual screening. Aminoacyl-tRNA synthetases are well expressed in the soluble form and can be used for high-throughput screening. Threonyl-tRNA synthetase (ThrRS) is a promising molecular target for malaria treatment.<sup>21,22</sup> For

Received: July 16, 2021

Published: September 16, 2021



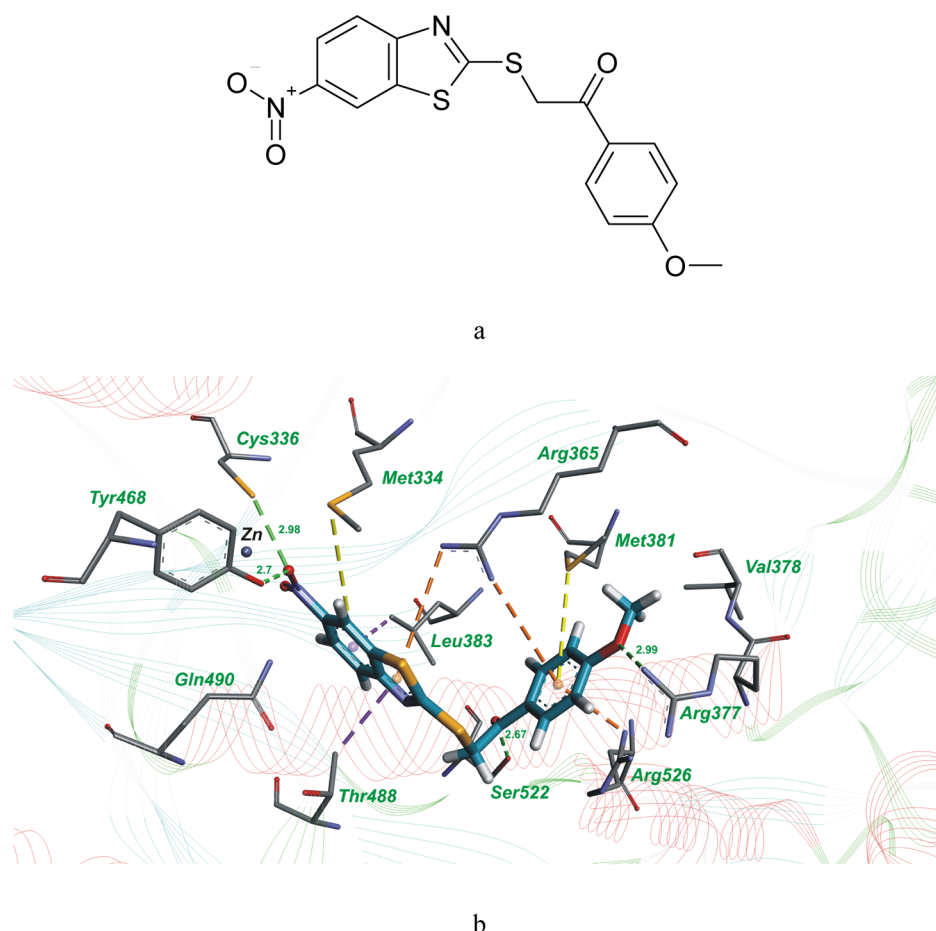


**Figure 1.** Chemical structure of 1-(4-methoxy-phenyl)-2-(6-nitro-benzothiazol-2-ylsulfanyl)-ethanone (compound 1) (a). The complex of compound 1 with amino acid residues in the active site of *S. aureus* ThrRS. The hydrogen bonds are shown by green dashed lines with the distances indicated in Å, the hydrophobic interactions are presented by magenta dashed lines,  $\pi$ -sulfur interactions are shown by yellow dashed lines, and  $\pi$ -cation interactions are indicated with orange dashed lines (b).

example, borrelidin, polyketide macrolide, isolated from *Streptomyces* species, is a potent inhibitor of ThrRS from *Plasmodium falciparum*.<sup>23,24</sup> Due to high toxicity of this compound, a series of borrelidin derivatives with lower toxicity has been synthesized.<sup>22,25,26</sup> The inhibitors of ThrRS from *Haemophilus influenzae*, *Escherichia coli*, and *Burkholderia thailandensis* possessing antibacterial activity have been reported among sulfonamide derivatives.<sup>27</sup> Recently, the inhibitors of *Salmonella enterica* ThrRS among quinazolinone derivatives have been identified using fragment-based target hopping assay by Guo et al.<sup>28</sup> The most active compound demonstrates an  $IC_{50}$  value of 1.4  $\mu$ M toward *Salmonella enterica* ThrRS. It should be noted that this compound revealed antibacterial activity toward *Escherichia coli* ATCC25922 and *S. enterica* with an MIC value of 16  $\mu$ g/mL and toward *S. aureus* ATCC29213, *S. aureus* R3708, and *Enterococcus faecalis* ATCC29212 with an MIC value of 32  $\mu$ g/mL.<sup>28</sup> Furthermore, these authors performed structure-based optimization of quinazolinone-threonine hybrids and discovered the inhibitor of *S. enterica* ThrRS with an  $IC_{50}$  value of 0.5  $\mu$ M and MIC values of 16–32  $\mu$ g/mL toward the tested bacterial strains.<sup>29</sup>

For the best of our knowledge, none of the small-molecular inhibitors of ThrRS from *S. aureus* have been reported in scientific literature so far. Therefore, the aim of this study is to obtain recombinant *S. aureus* ThrRS and identify inhibitors of

this enzyme with molecular docking into the available crystal structure of ThrRS.<sup>30</sup>

## RESULTS AND DISCUSSION

**Cloning and Purification of *S. aureus* Threonyl-tRNA Synthetase.** The gene encoding *S. aureus* ThrRS (1938 bp) with restriction sites for NcoI and HindIII was synthesized by ATG/biosynthetics GmbH (Merzhausen, Germany). To obtain the required amount of the *S. aureus* ThrRS gene for ligation, we performed preparative restriction of 5  $\mu$ g of plasmid DNA pGE-ThrRS(NcoI-HindIII) from the clones of *E. coli* Top10 cells with NcoI and HindIII. The linear DNA fragment was purified from gel using the NucleoSpin gel extraction kit (Macherey-Nagel) protocol.

The ThrRS gene fragment was ligated with a dephosphorylated vector pET28b linearized with NcoI and HindIII. *E. coli* cells TOP10 were electroporated with the plasmid pET28b-ThrRS. Plasmid DNA of clones with the correct fragments was prepared with a GeneJET Plasmid Miniprep Kit (Thermo Scientific). Transformation efficiency was analyzed with NcoI and HindIII. All tested plasmids contained a fragment of the expected size.

The most optimal conditions for expression of recombinant *S. aureus* ThrRS in the soluble fraction are the following: *E. coli* BL21(DE3)pLysS cells in LB medium, with induction by 0.25 mM isopropyl  $\beta$ -D-1-thiogalactopyranoside (IPTG) for 3 h at

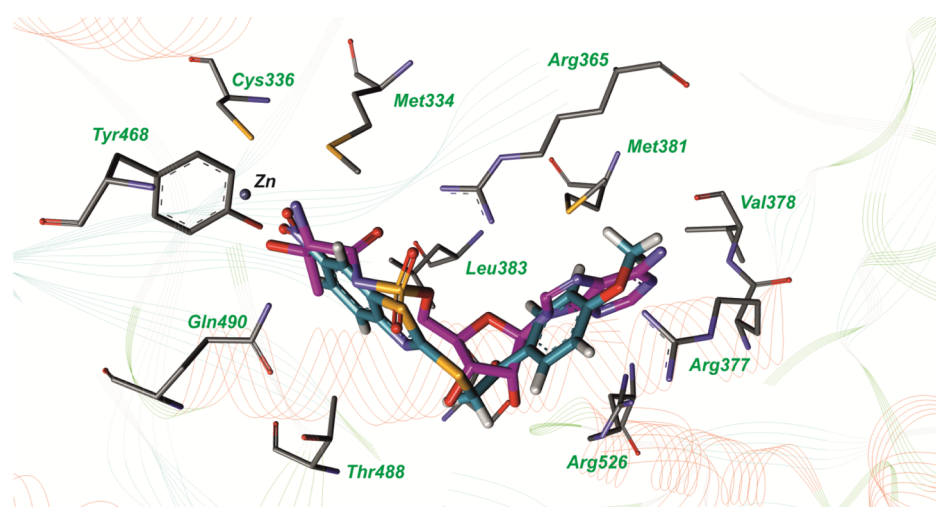


**Figure 2.** Superposition of the threonyl adenylate analogue, extracted from the crystal structure with the PDB accession code: 1NYQ (carbon atoms are labeled with magenta color) and compound 1 (carbon atoms are labeled with blue color) in the active site of *S. aureus* threonyl-tRNA synthetase.

37 °C or *E. coli* Lemo21(DE3) cells in 2YT medium supplemented with 250  $\mu\text{M}$  L-rhamnose at 30 °C during 16–18 h. The procedure for selection of optimal expression conditions for *S. aureus* ThrRS is available in [Supporting Information](#) (Figures S1–S10).

The protein was purified by DEAE Sepharose anion chromatography using a salt gradient from 25 to 500 mM NaCl (Figures S11, S12). The resulting eluate was concentrated and loaded onto a pre-equilibrated Heparin Sepharose 6 Fast Flow column and then eluted using the KCl gradient (from 0 to 300 mM) (Figure S13). The protein was concentrated to 3.5 mg/mL and stored with 50% glycerol at  $-80$  °C. The total yield of purified ThrRS (>95% purity) is 10 mg from 1 L starting bacterial culture. This protocol of purification was used for obtaining the required amount of recombinant *S. aureus* ThrRS for compound screening.

**Rational Design of *S. aureus* ThrRS Inhibitors.** In order to identify small-molecular inhibitors of *S. aureus* ThrRS, we have performed molecular docking of OTAVA compound library containing 124,831 compounds.<sup>31</sup> According to molecular docking results, we have selected 180 compounds for investigation of their inhibitory activity toward *S. aureus* ThrRS in an aminoacylation assay. The inhibitory activity for all tested compounds (%) (measured at least in duplicates) is available in [Supporting Information](#) (Table S1). Among the tested compounds, we identified active compounds belonging to five chemical classes—the derivatives of 2-(benzothiazol-2-ylsulfanyl)-1-phenyl-ethanone, 2-phenoxy-*N*-phenyl-acetamide, 4-phenyl-2-propionylamino-thiophene-3-carboxylic acid ethyl ester, 1-phenyl-pyrrolidine-2,5-dione, and *N*-benzylidene-*N'*-(4-phenyl-thiazol-2-yl)-hydrazine.

The compound 1-(4-methoxy-phenyl)-2-(6-nitro-benzothiazol-2-ylsulfanyl)-ethanone (compound 1) inhibits *S. aureus* ThrRS by 88.47% at a concentration of 100  $\mu\text{M}$ . The  $\text{IC}_{50}$  value for this compound is  $158 \pm 72$   $\mu\text{M}$  (measured in duplicates). According to molecular docking results, this compound interacts simultaneously with adenine-binding and amino acid-binding regions of ThrRS (Figure 1). The superposition of compound 1 and the threonyl adenylate analogue, extracted from the crystal structure of ThrRS (PDB ID: 1NYQ), in the active site is presented in Figure 2. As it can

be seen in Figure 1, 4-methoxy-phenyl interacts with amino acid residues in the adenine-binding site and forms a hydrogen bond with Arg377, the benzothiazol ring interacts with the amino acid residues in the threonyl-binding region, and the nitro group at the C6 position of this heterocycle builds hydrogen bonds with Cys336 and Tyr468.

In the present study, we tested six derivatives of 2-phenoxy-*N*-phenyl-acetamide for inhibitory activity toward *S. aureus* ThrRS. As it can be noticed from Table 1, the most active compound 2-(2-*tert*-butyl-phenoxy)-*N*-(2-methyl-5-nitro-phenyl)-acetamide (compound 2) inhibits *S. aureus* ThrRS by 85.59% at a concentration of 100  $\mu\text{M}$ . According to molecular docking results, *tert*-butyl of this compound interacts with the amino acid residues in the adenine-binding region of ThrRS, the nitro-phenyl ring interacts with the amino acid residues in the threonyl-binding region, and the nitro group forms the metal-acceptor bond with Zn (Figure 3).

We have made superposition of the most active compounds 1 and 2 in the aminoacyl-adenylate binding site of ThrRS (Figure S14). It was found that these ligands have a similar binding mode. Both compounds 1 and 2 interact simultaneously with adenine- and threonyl-binding regions and form  $\pi$ -cation interactions with the same residues Arg365 and Arg526. Possibly, the formation of hydrogen bonds of the nitro group in compound 1 is more profitable for inhibitory activity than the formation of the metal-acceptor bond of the nitro group in compound 2 with Zn.

In this research, three derivatives of 4-phenyl-2-propionylamino-thiophene-3-carboxylic acid ethyl ester were tested for inhibitory activity toward *S. aureus* ThrRS. As it can be seen from Table 2, the most active compound—4-(4-chloro-phenyl)-2-[2-(2,6-dimethyl-morpholin-4-yl)-acetyl-amino]-thiophene-3-carboxylic acid ethyl ester (compound 8), inhibits *S. aureus* ThrRS by 78.33%. According to molecular docking results, 2,6-dimethyl-morpholine heterocycle of this compound interacts with the amino acid residues in the adenine-binding region of ThrRS and forms a hydrogen bond with Arg377 and 4-chloro-phenyl interacts with the threonyl-binding region (Figure 4).

Among the investigated compounds, we have found two inhibitors of *S. aureus* ThrRS belonging to 1-phenyl-

**Table 1. Structures and *In Vitro* Inhibitory Activity of 2-Phenoxy-*N*-phenyl-acetamide Derivatives toward *S. aureus* ThrRS**

Nº	Structure	Residual activity of ThrRS, %
2		14.41
3		47.98
4		48.85
5		51.9
6		64.35
7		68.94

pyrrolidine-2,5-dione derivatives (Table 3). The compound 2-[1-(4-iodo-2-methyl-phenyl)-2,5-dioxo-pyrrolidin-3-ylsulfanyl]-nicotinic acid (compound 11) inhibits ThrRS by 78.62% at a concentration of 100  $\mu$ M. According to molecular docking results, the nicotinic acid moiety of this compound interacts with the adenine-binding region of ThrRS and forms a

**Table 2. Structures and *In Vitro* Inhibitory Activity of 4-Phenyl-2-propionylamino-thiophene-3-carboxylic Acid Ethyl Ester Derivatives toward *S. aureus* ThrRS**

Nº	Structure	Residual activity of ThrRS, %
8		21.67
9		25.01
10		53.52

hydrogen bond with Arg377 and 1-iodo-3-methyl-phenyl is located in the threonyl-binding region (Figure 5).

According to biochemical testing, *N*-benzylidene-*N'*-(4-phenyl-thiazol-2-yl)-hydrazine derivatives possess inhibitory activity toward *S. aureus* ThrRS. It should be noted that earlier, the compounds from this chemical class were reported by us as the inhibitors of *M. tuberculosis* leucyl-tRNA synthetase and methionyl-tRNA synthetase.<sup>32,33</sup> Therefore, the derivatives of *N*-benzylidene-*N'*-(4-phenyl-thiazol-2-yl)-hydrazine inhibit both classes of aminoacyl-tRNA synthetases.

As it can be seen from Table 4, among the 13 tested *N*-benzylidene-*N'*-(4-phenyl-thiazol-2-yl)-hydrazine derivatives, the most active compound –2,4-dibromo-6-[[4-(4-nitrophenyl)-thiazol-2-yl]-hydrazonomethyl]-phenol (compound 13) inhibits ThrRS by 72.65%. The IC<sub>50</sub> value for this

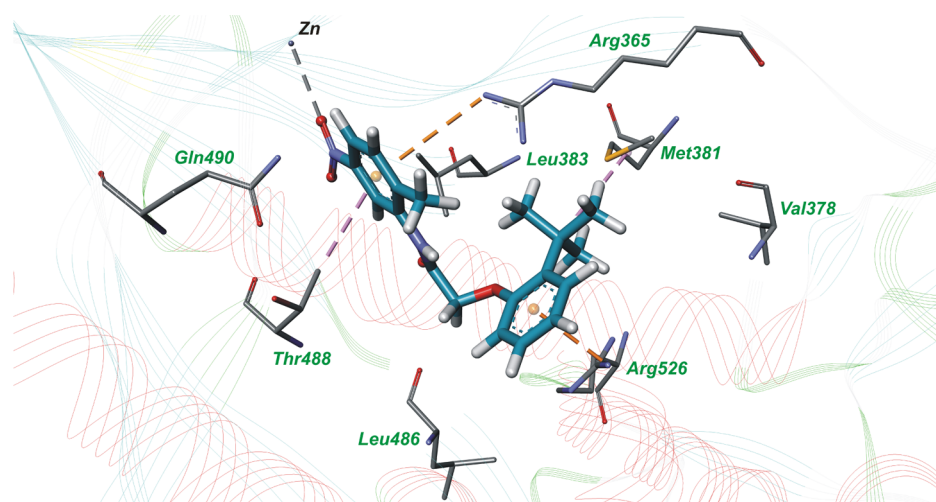


**Figure 3.** Complex of 2-(2-*tert*-butyl-phenoxy)-*N*-(2-methyl-5-nitro-phenyl)-acetamide (compound 2) with amino acid residues in the active site of *S. aureus* ThrRS. The hydrophobic interactions are indicated with magenta dashed lines,  $\pi$ -cation interactions are shown by orange dashed lines, and the metal-acceptor bond is presented by the gray dashed line.

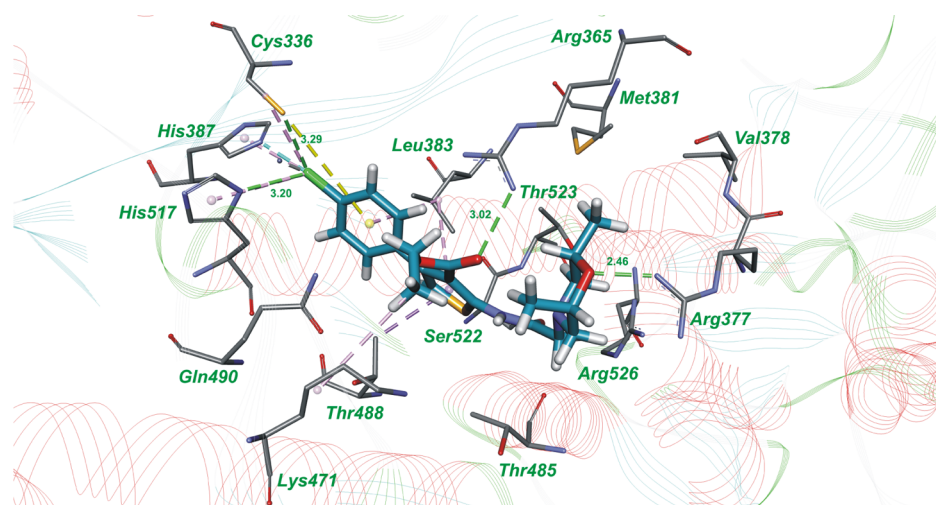


**Figure 4.** Complex of 4-(4-chloro-phenyl)-2-[2-(2,6-dimethyl-morpholin-4-yl)-acetylamino]-thiophene-3-carboxylic acid ethyl ester (compound **8**) with amino acid residues in the active site of *S. aureus* ThrRS. The hydrogen bonds are shown by green dashed lines with the distances indicated in Å, the hydrophobic interactions are indicated with magenta dashed lines,  $\pi$ -sulfur interaction is presented by yellow dashed lines, and the halogen bond is shown by blue dashed lines.

**Table 3. Structures and *In Vitro* Inhibitory Activity of 1-Phenyl-pyrrolidine-2,5-dione Derivatives toward *S. aureus* ThrRS**

No	Structure	Residual activity of ThrRS, %
11		21.38
12		56.32

compound is  $56.5 \pm 3.5 \mu\text{M}$  (measured in duplicates). Molecular docking results demonstrate that nitro-phenyl interacts with the amino acid residues in the threonyl-binding region of ThrRS and 2,4-dibromophenyl is located in the adenine-binding region of *S. aureus* ThrRS (Figure 6).

We have tested five hit compounds for cytotoxicity toward the human cell line HEK293 using standard MTT assay.<sup>34</sup> It was found that compounds **1**, **2**, **8**, and **13** are not cytotoxic at a concentration of  $100 \mu\text{M}$  and only compound **11** reveals slight toxicity, decreasing the growth of HEK293 cells by 30% at a concentration of  $100 \mu\text{M}$  ( $\text{EC}_{50} > 100 \mu\text{M}$ ).

## CONCLUSIONS

Using the rational design approach, we identified five hit compounds from different chemical classes, inhibiting *S. aureus* threonyl-tRNA synthetase (ThrRS) by more than 70% at a concentration of  $100 \mu\text{M}$ . The most active compound 2,4-dibromo-6-[[4-(4-nitro-phenyl)-thiazol-2-yl]-hydrazonomethyl]-phenol has an  $\text{IC}_{50}$  value of  $56.5 \pm 3.5 \mu\text{M}$ . According to the results of molecular docking, the inhibitors interact

simultaneously with adenine- and threonyl-binding regions of *S. aureus* ThrRS. These compounds are not cytotoxic toward the human cell line HEK293 and can be used for further chemical optimization and biological research. It should be noted that the derivatives of *N*-benzylidene-*N'*-(4-phenyl-thiazol-2-yl)-hydrazine inhibit both classes of aminoacyl-tRNA synthetases from different microorganisms and can be considered for the development of broad spectrum antibiotics.

## METHODS

**Molecular Docking.** Semiflexible molecular docking of the small-molecular compounds into the active site of the *S. aureus* ThrRS crystal structure (PDB ID: 1NYQ) was performed with the program DOCK 4.0.<sup>35–38</sup> The molecules of 5'-*O*-(*N*-(1-threonyl)-sulfamoyl)adenosine and water were removed from the crystal structure, but the Zn ion was kept in the active site.

The ligand geometry was calculated using the YFF force field.<sup>39</sup> The partial atomic charges for the ligands were assigned with the Kirchhoff method.<sup>40</sup> The partial atomic charges for the receptor were set with the Amber force field. The spheres of the active site were predicted using sphgen software from the DOCK package. The spheres which were outside of the aminoacyl-adenylate binding site of ThrRS were deleted manually. The energy grids of the receptor were generated using the grid program from the DOCK package.

The docking of the compound library into the aminoacyl-adenylate binding site of ThrRS was performed using the parameters described earlier.<sup>32</sup>

After the docking procedure, we have performed complex analysis to select compounds for *in vitro* screening. At first, compounds were ranged based on score values (less than  $-40$  kcal/mol). Then, the compounds were evaluated for the ability to form hydrogen bonds with amino acid residues in the aminoacyl adenylate binding site of *S. aureus* ThrRS, such as Tyr468, Met334, Gln490, Asp385, Arg365, Ser522, Thr523, and Val378 using our in-house program  $\gamma$ \_hbonds, which is based on the analysis of distances and angles between the respective donor and acceptor atoms. Considering these criteria, we have chosen about 12,000 compounds for further visual inspection of receptor–ligand complexes. During visual

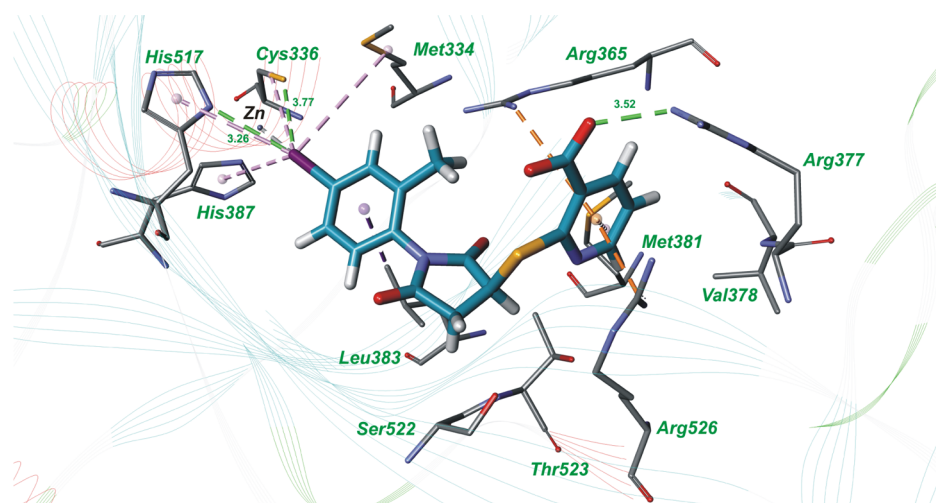


**Figure 5.** Complex of 2-[1-(4-iodo-2-methyl-phenyl)-2,5-dioxo-pyrrolidin-3-ylsulfanyl]-nicotinic acid (compound 11) with amino acid residues in the active site of *S. aureus* ThrRS. The hydrogen bonds are shown by green dashed lines with the distances indicated in Å, the hydrophobic interactions are presented by magenta dashed lines,  $\pi$ -cation interactions are indicated with orange dashed lines, and the metal-acceptor bond is shown by gray dashed lines.

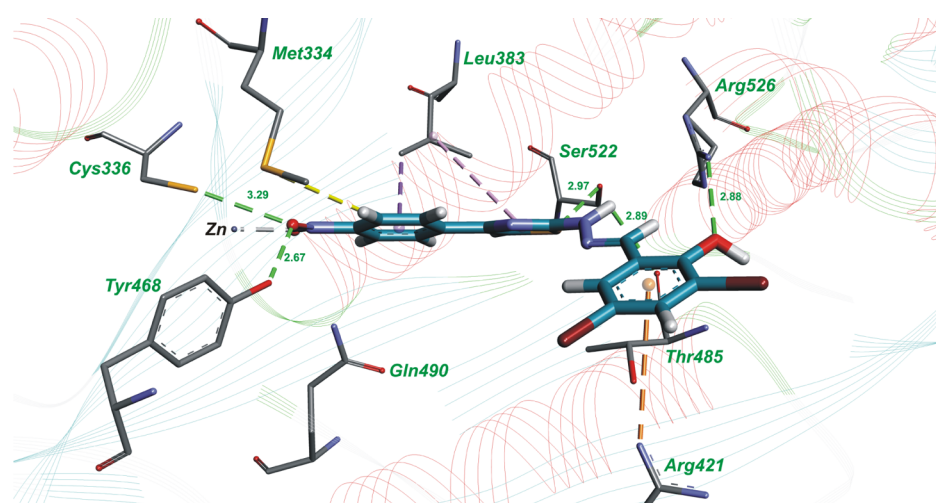


**Figure 6.** Complex of 2,4-dibromo-6-[[4-(4-nitro-phenyl)-thiazol-2-yl]-hydrazonomethyl]-phenol (compound 13) with amino acid residues in the active site of *S. aureus* ThrRS. The hydrogen bonds are shown by green dashed lines with the distances indicated in Å, the hydrophobic interactions are presented by magenta dashed lines,  $\pi$ -cation interaction is indicated with orange dashed lines,  $\pi$ -sulfur interaction is presented by yellow dashed lines, and the metal-acceptor bond is shown by gray dashed lines.

analysis, we evaluated correctness of torsion angles, stacking interactions, complementarity of ligand and receptor surfaces, and so forth. Taking into account all these parameters, we have selected 180 compounds for investigation of their inhibitory activity toward recombinant *S. aureus* ThrRS.

Visual analysis of the receptor–ligand complexes was performed using Discovery Studio Visualizer 4.0.<sup>41</sup>

**Cloning of ThrRS.** The gene encoding ThrRS with restriction sites for NcoI and HindIII was synthesized by ATG/biosynthetics GmbH (Merzhausen, Germany) based on sequence information of the *S. aureus* ThrRS gene (GenBank ID: ABD30857.1). The linearized DNA fragment pGE(NcoI-HindIII)-ThrRS-S was ligated to the plasmid vector pET28b (Novagen) which was previously dephosphorylated with phosphatase in 1× reaction buffer (Roche). Ligation was performed with T4 DNA ligase in 1× ligase buffer (Promega) for 2 h at 23 °C. *E. coli* TOP10 cells (Invitrogen) were transformed by electroporation using a Bio-Rad Gene Pulsar.

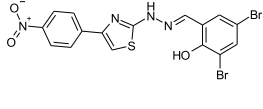
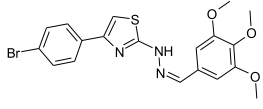
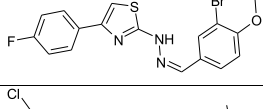
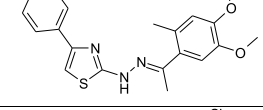
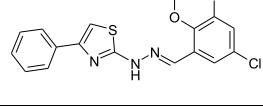
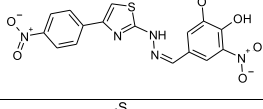
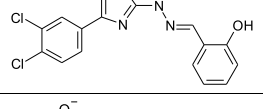
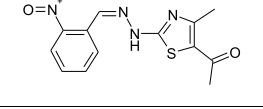
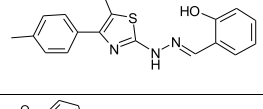
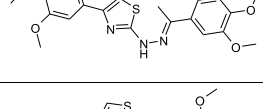
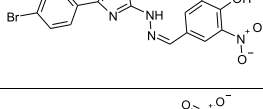
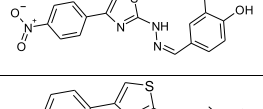
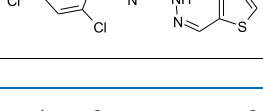
The screening of positive clones was performed using the GeneJET Plasmid Miniprep Kit (Thermo Scientific). Positive clones were identified using restrictases NcoI and HindIII FastDigest (Thermo Scientific).

**ThrRS Expression.** The plasmid pET28b-ThrRS was transformed into *E. coli* BL21(DE3)pLysS and Lemo21(DE3) competent cells. The level of expression was analyzed in LB (Lauria-Broth), TB (Terrific-Broth), phosphate, and 2×YT media with 50  $\mu$ g/mL kanamycin. The bacterial growth was continued until the OD<sub>600</sub> reached around 0.6. The protein synthesis was induced by IPTG in the range of concentration from 0.025 mM to 1 mM at 18, 25, and 37 °C.

Aliquots after 3–4 h and overnight induction were analyzed for solubility according to the protocol of Zerbs et al.<sup>42</sup>

For ThrRS expression, a modified<sup>43</sup> autoinduction protocol<sup>44</sup> was also used. *E. coli* BL21(DE3)pLysS and Lemo21-(DE3) cells harboring the plasmid pET28b-ThrRS were incubated at 37 °C overnight in 2 mL of 2×YT medium

**Table 4. Structures and *In Vitro* Inhibitory Activity of *N*-Benzylidene-*N'*-(4-phenyl-thiazol-2-yl)-hydrazine Derivatives toward *S. aureus* ThrRS**

No	Structure	Residual activity of ThrRS, %
13		27.35 (IC <sub>50</sub> = 56.5 ± 3.5 μM)
14		37.97
15		45.32
16		46.71
17		46.98
18		52.15
19		54.58
20		55.73
21		57.10
22		57.67
23		76.31
24		80.93
25		128.48

containing 50 μg/mL kanamycin and 1% glucose. 1:1000 dilutions of the overnight culture were taken for inoculation of 2×YT medium supplemented with 40 μg/mL kanamycin, 25 mM (NH<sub>4</sub>)<sub>2</sub>SO<sub>4</sub>, 50 mM KH<sub>2</sub>PO<sub>4</sub>, 50 mM Na<sub>2</sub>HPO<sub>4</sub>, 1 mM

MgSO<sub>4</sub>, 0.05% glucose, 0.2% α-lactose, and 0.5% glycerol. The cultures were incubated at 18/30/37 °C for 16–18 h under conditions of intensive aeration.

**Purification of *S. aureus* ThrRS.** *E. coli* cells BL21(DE3)-pLysS were grown in the medium LB until the OD<sub>600</sub> reached 0.6, and the expression of ThrRS was induced by 0.25 mM IPTG for 3 h at 37 °C. The cells were pelleted by centrifugation (15 min at 6000 g at 4 °C), and the pellets were stored at –80 °C. The bacterial pellet was dissolved in buffer A containing 100 mM Tris-HCl (pH 8.0), 300 mM NaCl, 10 mM DTT, 5 mM PMSF, 4% glycerol, 1 mM MgCl<sub>2</sub>, 0.01 mg/mL lysozyme, and protease inhibitor cocktail tablet, EDTA-free. The cells were incubated on ice for 30 min and sonicated for 5 min with four sonicated bursts of 25 s followed by interval of 60 s for cooling. The cell pellet was precipitated by centrifugation at 20000g for 25 min at 4 °C. The supernatant was dialyzed in buffer B containing 20 mM Tris-HCl (pH 8.0), 2 mM DTT, 0.1 mM PMSF, and 5 mM MgCl<sub>2</sub> for 3 h at 4 °C. Then, the buffer was changed and dialyzed overnight. After dialysis, the lysate was loaded onto a DEAE Sepharose column (Amersham Biosciences) (*V* = 6.5 mL), washed at a flow rate of 1 mL/min, and eluted with a gradient of NaCl from 25 to 500 mM (2 × 50 mL). Fractions were analyzed by the Bradford method<sup>45</sup> and SDS-PAGE. Fractions containing ThrRS were joined and concentrated on an Amicon Ultra-4 at 10 K MWCO spin column (Millipore, Billerica, MA) at 4 °C to remove salt impurities and loaded onto the Heparin Sepharose 6 Fast Flow column (GE Healthcare) (0.5 × 10 cm), washed with buffer B and eluted with a gradient of KCl from 0 to 300 mM (2 × 25 mL). The peak fractions, containing ThrRS, were joined and concentrated on Amicon Ultra-4 (7000 g, 4 °C).

Protein concentrations were determined by the Bradford method.<sup>45</sup> The absorption coefficient at λ = 280 nm ( $\epsilon_{280} = 73355 \text{ M}^{-1} \text{ cm}^{-1}$ ) and the absorption of 0.1% solution ( $A_{280} (1 \text{ mg/mL}) = 0.985 \text{ mg}^{-1} \text{ mL}$ ) were calculated from the *S. aureus* ThrRS amino acid sequence using the ExpASY ProtParam tool<sup>46</sup> and taken for determination of enzyme concentration.

***In Vitro* Aminoacylation Assay.** The standard aminoacylation assay was performed in the reaction mixture (20 μM) containing 50 mM HEPES-NaOH (pH 7.5), 20 mM MgCl<sub>2</sub>, 5 mM β-mercaptoethanol, 30 mM KCl, 100 μg/mL BSA, 4 mg/mL of the total *E. coli* MRE600 tRNA, 27 μM [<sup>14</sup>C]-L-Thr, and 500 nM recombinant *S. aureus* ThrRS with appropriate concentrations of the compound (dissolved in DMSO). The reactions were initiated by the addition of 10 mM ATP and incubated for 10 min at 37 °C. The reaction was stopped by the addition of 10% trichloroacetic acid and was loaded on the GF/C filter, washed with 5% trichloroacetic acid, dried, and counted using a scintillation counter. Aliquots were quenched with 10% trichloroacetic acid, and the level of tRNA aminoacylation was measured using a scintillation counter [Hidex 600 SL liquid scintillation analyzer (Finland)].

**MTT Assay.** The toxicity of compounds toward the HEK293 cell was examined using a standard MTT assay.<sup>35</sup> The cells were cultivated in Dulbecco's modified Eagle's medium supplemented with 10% fetal bovine serum, 100 mg/mL streptomycin, and 100 mg/mL penicillin in humidified air with 5% CO<sub>2</sub> at 37 °C. The cells were seeded into 96-well plates at a concentration of 2 × 10<sup>5</sup> cells/mL and grown for 24 h. Then, the cells were supplemented with compounds in DMSO solution (final DMSO concentration was less than 0.5%) at different concentrations. After 72 h of incubation, the

cells were treated with 15  $\mu$ L of MTT solution (5 mg/mL) for 4 h at 37  $^{\circ}$ C, 5% CO<sub>2</sub>. The formazan precipitates were dissolved in 200  $\mu$ L of DMSO, and the absorbance at  $\lambda$  = 540 nm was measured with spectrofluorometer MR 700 (Dynatech). The cell viability was calculated as a percentage relative to intact control cells.

## ■ ASSOCIATED CONTENT

### SI Supporting Information

The Supporting Information is available free of charge at <https://pubs.acs.org/doi/10.1021/acsomega.1c03789>.

Analysis of ThrRS expression in *E. coli* BL21(DE3)-pLysS cells; analysis of expression of the ThrRS soluble fraction with induction by 0.5 or 1 mM IPTG concentrations at 37  $^{\circ}$ C; analysis of expression of the ThrRS soluble fraction with induction by 0.25, 0.5, or 1 mM IPTG concentrations at 25  $^{\circ}$ C; analysis of ThrRS expression at 0.1 and 0.25 mM IPTG concentration and in the medium with 3% ethanol after induction for 3 h at 37  $^{\circ}$ C; expression of the ThrRS soluble fraction with induction by 0.1, 0.25, and 1 mM IPTG concentration and in the medium with 3% ethanol for 3 h at 18 and 25  $^{\circ}$ C; expression of the ThrRS soluble fraction after overnight induction at 18 and 25  $^{\circ}$ C; expression of the ThrRS soluble fraction in Lemo21(DE3) *E. coli* cells in LB medium after 4 h of induction at 30  $^{\circ}$ C with 0.4 mM IPTG and various concentrations of L-rhamnose; expression of the ThrRS soluble fraction in Lemo21(DE3) *E. coli* cells in LB medium after overnight induction at 30  $^{\circ}$ C; expression of *S. aureus* ThrRS using the autoinduction protocol; SDS-PAGE analysis of soluble and insoluble fractions of *E. coli* proteins after induction expression of *S. aureus* ThrRS by autoinduction conditions (10  $\mu$ L of culture per lane was loaded); elution profile (absorbance at 280 nm versus elution volume) of the anion exchanger DEAE-Sepharose; purification of *S. aureus* ThrRS using the DEAE-Sepharose column; purification of *S. aureus* ThrRS using the heparin-Sepharose column; superposition of compound 1 (carbon atoms are labeled with blue color) and compound 2 (carbon atoms are labeled with magenta color) in the active site of *S. aureus* threonyl-tRNA synthetase; and structures and *in vitro* inhibitory activity toward *S. aureus* ThrRS for compounds, selected according to molecular docking results (PDF)

## ■ AUTHOR INFORMATION

### Corresponding Author

**Galyna P. Volynets** – Department of Medicinal Chemistry, Institute of Molecular Biology and Genetics National Academy of Sciences of Ukraine, Kyiv 03143, Ukraine; The Scientific-Services Company “OTAVA”, Kyiv 03143, Ukraine; [orcid.org/0000-0002-0166-2642](https://orcid.org/0000-0002-0166-2642); Email: [g.p.volynets@gmail.com](mailto:g.p.volynets@gmail.com)

### Authors

**Mariia Yu. Rybak** – Department of Protein Synthesis Enzymology, Institute of Molecular Biology and Genetics National Academy of Sciences of Ukraine, Kyiv 03143, Ukraine; [orcid.org/0000-0002-0478-0222](https://orcid.org/0000-0002-0478-0222)

**Olga I. Gudzera** – Department of Protein Synthesis Enzymology, Institute of Molecular Biology and Genetics National Academy of Sciences of Ukraine, Kyiv 03143, Ukraine

**Oksana B. Gorbatyuk** – Department of Cell Regulatory Mechanisms, Institute of Molecular Biology and Genetics National Academy of Sciences of Ukraine, Kyiv 03143, Ukraine

**Mariia O. Usenko** – Department of Cell Regulatory Mechanisms, Institute of Molecular Biology and Genetics National Academy of Sciences of Ukraine, Kyiv 03143, Ukraine

**Sergiy M. Yarmoluk** – Department of Medicinal Chemistry, Institute of Molecular Biology and Genetics National Academy of Sciences of Ukraine, Kyiv 03143, Ukraine

**Michael A. Tukalo** – Department of Protein Synthesis Enzymology, Institute of Molecular Biology and Genetics National Academy of Sciences of Ukraine, Kyiv 03143, Ukraine

Complete contact information is available at: <https://pubs.acs.org/doi/10.1021/acsomega.1c03789>

### Notes

The authors declare no competing financial interest.

## ■ ACKNOWLEDGMENTS

This work was supported by the NAS of the Ukraine grant for young scientists (project no 0120U000079) for 2020–2021.

## ■ REFERENCES

- (1) Krishna, S.; Miller, L. S. Host-pathogen interactions between the skin and *Staphylococcus aureus*. *Curr. Opin. Microbiol.* **2012**, *15*, 28–35.
- (2) Welte, T.; Kantecki, M.; Stone, G. G.; Hammond, J. Ceftaroline fosamil as a potential treatment option for *Staphylococcus aureus* community-acquired pneumonia in adults. *Int. J. Antimicrob. Agents* **2019**, *54*, 410–422.
- (3) Jang, Y.-R.; Kim, T.; Kim, M.-C.; Sup Sung, H.; Kim, M.-N.; Kim, M. J.; Kim, S. H.; Lee, S.-O.; Choi, S.-H.; Woo, J. H.; Kim, Y. S.; Chong, Y. P. Sternoclavicular septic arthritis caused by *Staphylococcus aureus*: excellent results from medical treatment and limited surgery. *Infect. Dis.* **2019**, *51*, 694–700.
- (4) Tascini, C.; Attanasio, V.; Ripa, M.; Carozza, A.; Pallotto, C.; Bernardo, M.; Francisci, D.; Oltolini, C.; Palmiero, G.; Scarpellini, P. Cefotaxime for the treatment of infective endocarditis: a case series. *J. Glob. Antimicrob. Resist.* **2020**, *20*, 56–59.
- (5) Dugourd, P.-M.; Dupont, A.; Hubiche, T.; Chiaverini, C.; Alkhalifa, A.; Roudiere, L.; Tristan, A.; Gustave, C.-A.; Del Giudice, P. Érythème généralisé fébrile et choc : choc toxique staphylococcique. *Ann. Dermatol. Venereol.* **2019**, *146*, 287–291.
- (6) Toledo, A. G.; Golden, G.; Campos, A. R.; Cuello, H.; Sorrentino, J.; Lewis, N.; Varki, N.; Nizet, V.; Smith, J. W.; Esko, J. D. Proteomic atlas of organ vasculopathies triggered by *Staphylococcus aureus* sepsis. *Nat. Commun.* **2019**, *10*, 4656.
- (7) Bergin, S. P.; Holland, T. L.; Fowler, V. G., Jr.; Tong, S. Y. C. Bacteremia, sepsis, and infective endocarditis associated with *Staphylococcus aureus*. *Curr. Top. Microbiol. Immunol.* **2015**, *409*, 263–296.
- (8) Zhang, Y.; Zhang, J.; Chen, W.; Angsantikul, P.; Spiekermann, K. A.; Fang, R. H.; Gao, W.; Zhang, L. Erythrocyte membrane-coated nanogel for combinatorial antivirulence and responsive antimicrobial delivery against *Staphylococcus aureus* infection. *J. Controlled Release* **2017**, *263*, 185–191.
- (9) Gardete, S.; Tomasz, A. Mechanisms of vancomycin resistance in *Staphylococcus aureus*. *J. Clin. Invest.* **2014**, *124*, 2836–2840.



- (10) Kali, A. Antibiotics and bioactive natural products in treatment of methicillin resistant *Staphylococcus aureus*: A brief review. *Pharmacogn. Rev.* **2015**, *9*, 29–34.
- (11) Kaur, D.; Chate, S. Study of antibiotic resistance pattern in methicillin resistant *staphylococcus aureus* with special reference to newer antibiotic. *J. Global Infect. Dis.* **2015**, *7*, 78–84.
- (12) Arunkumar, V.; Prabagaravathanan, R.; Bhaskar, M. Prevalence of methicillin-resistant *Staphylococcus aureus* (MRSA) infections among patients admitted in critical care units in a tertiary care hospital. *Int. J. Res. Med. Sci.* **2017**, *5*, 2362–2366.
- (13) McGuinness, W. A.; Malachowa, N.; DeLeo, F. R. Vancomycin Resistance in *Staphylococcus aureus*. *Yale J. Biol. Med.* **2017**, *90*, 269–281.
- (14) Marty, F. M.; Yeh, W. W.; Wennersten, C. B.; Venkataraman, L.; Albano, E.; Alyea, E. P.; Gold, H. S.; Baden, L. R.; Pillai, S. K. Emergence of a clinical daptomycin-resistant *Staphylococcus aureus* isolate during treatment of methicillin-resistant *Staphylococcus aureus* bacteremia and osteomyelitis. *J. Clin. Microbiol.* **2006**, *44*, 595–597.
- (15) Ikeda-Dantsuji, Y.; Hanaki, H.; Sakai, F.; Yanagisawa, C.; Nakae, T.; Sakai, F.; Tomono, K.; Takesue, Y.; Honda, J.; Nonomiya, Y.; Suwabe, A.; Nagura, O.; Yanagihara, K.; Mikamo, H.; Fukuchi, K.; Kaku, M.; Kohno, S.; Yoshida, K.; Niki, Y. Linezolid-resistant *Staphylococcus aureus* isolated from 2006 through 2008 at six hospitals in Japan. *J. Infect. Chemother.* **2011**, *17*, 45–51.
- (16) Pang, L.; Weeks, S. D.; Van Aerschot, A. Aminoacyl-tRNA synthetases as valuable targets for antimicrobial drug discovery. *Int. J. Mol. Sci.* **2021**, *22*, 1750.
- (17) Kwon, N. H.; Fox, P. L.; Kim, S. Aminoacyl-tRNA synthetases as therapeutic targets. *Nat. Rev. Drug Discovery* **2019**, *18*, 629–650.
- (18) Ho, J. M.; Bakkalbasi, E.; Söll, D.; Miller, C. A. Drugging tRNA aminoacylation. *RNA Biol.* **2018**, *15*, 667–677.
- (19) Ribas de Pouplana, L.; Schimmel, P. Two classes of tRNA synthetases suggested by sterically compatible dockings on tRNA acceptor stem. *Cell* **2001**, *104*, 191–193.
- (20) Eriani, G.; Delarue, M.; Poch, O.; Gangloff, J.; Moras, D. Partition of tRNA synthetases into two classes based on mutually exclusive sets of sequence motifs. *Nature* **1990**, *347*, 203–206.
- (21) Novoa, E. M.; Camacho, N.; Tor, A.; Wilkinson, B.; Moss, S.; Marín-García, P.; Azcarate, I. G.; Bautista, J. M.; Miranda, A. C.; Francklyn, C. S.; Varon, S.; Royo, M.; Cortés, A.; Ribas de Pouplana, L. Analogs of natural aminoacyl-tRNA synthetase inhibitors clear malaria *in vivo*. *Proc. Natl. Acad. Sci. U.S.A.* **2014**, *111*, E5508–E5517.
- (22) Saint-Léger, A.; Sinadinos, C.; Ribas de Pouplana, L. The growing pipeline of natural aminoacyl-tRNA synthetase inhibitors for malaria treatment. *Bioengineered* **2016**, *7*, 60–64.
- (23) Hütter, R.; Poralla, K.; Zachau, H. G.; Zähner, H. Metabolic products of microorganisms. 51. On the mechanism of action of borrelidin-inhibition of the threonine incorporation in sRNA. *Biochem. Z.* **1966**, *344*, 190–196.
- (24) Paetz, W.; Nass, G. Biochemical and Immunological Characterization of Threonyl-tRNA Synthetase of Two Borrelidin-Resistant Mutants of *Escherichia coli* K12. *Eur. J. Med. Chem.* **1973**, *35*, 331–337.
- (25) Wilkinson, B.; Gregory, M. A.; Moss, S. J.; Carletti, I.; Sheridan, R. M.; Kaja, A.; Ward, M.; Olano, C.; Mendez, C.; Salas, J. A.; Leadlay, P. F.; van Ginckel, R.; Zhang, M.-Q. Separation of anti-angiogenic and cytotoxic activities of borrelidin by modification at the C17 side chain. *Bioorg. Med. Chem. Lett.* **2006**, *16*, 5814–5817.
- (26) Sugawara, A.; Tanaka, T.; Hirose, T.; Ishiyama, A.; Iwatsuki, M.; Takahashi, Y.; Otoguro, K.; Ōmura, S.; Sunazuka, T. Borrelidin analogues with antimalarial activity: design, synthesis and biological evaluation against *Plasmodium falciparum* parasites. *Bioorg. Med. Chem. Lett.* **2013**, *23*, 2302–2305.
- (27) Teng, M.; Hilgers, M. T.; Cunningham, M. L.; Borchardt, A.; Locke, J. B.; Abraham, S.; Haley, G.; Kwan, B. P.; Hall, C.; Hough, G. W.; Shaw, K. J.; Finn, J. Identification of bacteria-selective threonyl-tRNA synthetase substrate inhibitors by structure-based design. *J. Med. Chem.* **2013**, *56*, 1748–1760.
- (28) Guo, J.; Chen, B.; Yu, Y.; Cheng, B.; Cheng, Y.; Ju, Y.; Gu, Q.; Xu, J.; Zhou, H. Discovery of novel tRNA-amino acid dual-site inhibitors against threonyl-tRNA synthetase by fragment-based target hopping. *Eur. J. Med. Chem.* **2020**, *187*, 111941.
- (29) Guo, J.; Chen, B.; Yu, Y.; Cheng, B.; Ju, Y.; Tang, J.; Cai, Z.; Gu, Q.; Xu, J.; Zhou, H. Structure-guided optimization and mechanistic study of a class of quinazolinone-threonine hybrids as antibacterial ThrRS inhibitors. *Eur. J. Med. Chem.* **2020**, *207*, 112848.
- (30) Torres-Larios, A.; Sankaranarayanan, R.; Rees, B.; Dock-Bregeon, A.-C.; Moras, D. Conformational movements and cooperativity upon amino acid, ATP and tRNA binding in threonyl-tRNA synthetase. *J. Mol. Biol.* **2003**, *331*, 201–211.
- (31) We used a database of commercially available compounds; Otava Ltd., <http://www.otavachemicals.com>, (accessed April, 2020).
- (32) Kovalenko, O. P.; Volynets, G. P.; Rybak, M. Y.; Starosyla, S. A.; Gudzera, O. I.; Lukashov, S. S.; Bdzhol, V. G.; Yarmoluk, S. M.; Boshoff, H. I.; Tukalo, M. A. Dual-target inhibitors of mycobacterial aminoacyl-tRNA synthetases among N-benzylidene-N'-thiazol-2-yl-hydrazines. *Medchemcomm* **2019**, *10*, 2161–2169.
- (33) Gudzera, O. I.; Golub, A. G.; Bdzhol, V. G.; Volynets, G. P.; Lukashov, S. S.; Kovalenko, O. P.; Krikliivyi, I. A.; Yaremchuk, A. D.; Starosyla, S. A.; Yarmoluk, S. M.; Tukalo, M. A. Discovery of potent anti-tuberculosis agents targeting leucyl-tRNA synthetase. *Bioorg. Med. Chem.* **2016**, *24*, 1023–1031.
- (34) Mosmann, T. Rapid colorimetric assay for cellular growth and survival: application to proliferation and cytotoxicity assays. *J. Immunol. Methods* **1983**, *65*, 55–63.
- (35) Bodian, D. L.; Yamasaki, R. B.; Buswell, R. L.; Stearns, J. F.; White, J. M.; Kuntz, I. D. Inhibition of the fusion-inducing conformational change of influenza hemagglutinin by benzoquinones and hydroquinones. *Biochemistry* **1993**, *32*, 2967–2978.
- (36) Ewing, T. J. A.; Makino, S.; Skillman, A. G.; Kuntz, I. D. DOCK 4.0: search strategies for automated molecular docking of flexible molecule databases. *J. Comput.-Aided Mol. Des.* **2001**, *15*, 411–428.
- (37) Ring, C. S.; Sun, E.; McKerrow, J. H.; Lee, G. K.; Rosenthal, P. J.; Kuntz, I. D.; Cohen, F. E. Structure-based inhibitor design by using protein models for the development of antiparasitic agents. *Proc. Natl. Acad. Sci. U.S.A.* **1993**, *90*, 3583–3587.
- (38) Shoichet, B. K.; Stroud, R. M.; Santi, D. V.; Kuntz, I. D.; Perry, K. M. Structure-based discovery of inhibitors of thymidylate synthase. *Science* **1993**, *259*, 1445–1450.
- (39) Yakovenko, O. Y.; Oliferenko, A.; Golub, A.; Bdzhol, V.; Yarmoluk, S. The new method of distribution integrals evaluations for high throughput virtual screening. *Ukr. Bioorg. Acta* **2007**, *1*, 52–62.
- (40) Yakovenko, O.; Oliferenko, A. A.; Bdzhol, V. G.; Palyulin, V. A.; Zefirov, N. S. Kirchhoff atomic charges fitted to multipole moments: Implementation for a virtual screening system. *J. Comput. Chem.* **2008**, *29*, 1332–1343.
- (41) Discovery Studio Visualizer 4.0, 2019. <https://www.3dsbiovia.com/products/collaborative-science/biovia-discovery-studio/visualization-download.php>, (accessed May, 2019).
- (42) Zerbs, S.; Frank, A. M.; Collart, F. R. Chapter 12 Bacterial Systems for Production of Heterologous Proteins. *Methods Enzymol.* **2009**, *463*, 149–168.
- (43) Gorbatiuk, O. B.; Tsapenko, M. V.; Pavlova, M. V.; Okunev, O. V.; Kordium, V. A. Bioaffinity sorbent based on immobilized protein A *Staphylococcus aureus*: development and application. *Biopolym. Cell* **2012**, *28*, 141–148.
- (44) Studier, F. W. Protein production by auto-induction in high-density shaking cultures. *Protein Expression Purif.* **2005**, *41*, 207–234.
- (45) Bradford, M. M. A rapid and sensitive method for the quantitation of microgram quantities of protein utilizing the principle of protein-dye binding. *Anal. Biochem.* **1976**, *72*, 248–254.
- (46) Gasteiger, E.; Gattiker, A.; Hoogland, C.; Ivanyi, I.; Appel, R. D.; Bairoch, A. ExPASy: The proteomics server for in-depth protein knowledge and analysis. *Nucleic Acids Res.* **2003**, *31*, 3784–3788.